

# Finish turning of toolox 33 to improve machining parameters with different nose radius tools

Kübra Kaya<sup>1</sup> , Tayfun Çetin<sup>2\*</sup> , Rüstem Binali<sup>1</sup> , Hakan Gündoğmuş<sup>3</sup> 

<sup>1</sup> Selçuk University, Department of Mechanical Engineering, 42075, Konya, Türkiye

<sup>2</sup> Hakkari University, Department of Electricity and Energy, Yüksekova Vocational School, 30000, Hakkari, Türkiye

<sup>3</sup> Hakkari University, Department of Mechanical Engineering, 30000, Hakkari, Türkiye

**Abstract:** Turning, the most widely used machining process in manufacturing, continues to maintain its popularity today. Given its ongoing relevance, evaluating machinability in turning operations remains critical. In this study, dry turning was applied to Toolox 33, a material commonly used due to its favorable machinability characteristics. In the experimental research, changes in surface roughness and cutting force (two of the most critical output parameters) were evaluated in the context of machinability by applying different values of machining parameters, including tool nose radius, cutting speed, feed, and cutting depth. The investigation was undertaken with consideration of integrating machine learning methods into the manufacturing process. The results of the study indicated that optimal cutting force values can be achieved by employing a larger tool nose radius, higher cutting speeds, and lower feed rates and depths of cut. Similarly, optimal surface roughness was obtained under conditions involving a larger nose radius tool, lower feed, and shallower cutting depth. However, variations in the cutting speed parameter led to differing results in surface roughness. For instance, while an increase in cutting speed led to lower surface roughness values in some experimental sets, an increase in surface roughness was observed in others. Graphical evaluations confirmed the suitability of machine learning techniques for this application. The optimum cutting force was recorded under experimental conditions involving a 0.8 mm nose radius tool, a feed rate of 0.2 mm/rev, a depth of cut of 0.2 mm, and a cutting speed of 60 m/min. The best surface roughness results were obtained in the same experiment that yielded the optimum cutting force values. Compared to the optimum result obtained with a 0.8 mm nose radius tool, reducing the nose radius to 0.4 mm increased the cutting force by 29.87%, increasing the feed rate to 0.4 mm/rev led to a 100% rise, and increasing the depth of cut to 0.4 mm resulted in a 62.33% increase. In contrast, increasing the cutting speed from 40 m/min to 60 m/min reduced the cutting force by 44.20%. Following the physical experiments, it was observed that increasing the cutting speed from 40 to 60 m/min reduced surface roughness (Ra) by approximately 5% to 22%, while increasing the cutting depth from 0.2 mm to 0.4 mm and the feed rate from 0.2 mm/rev to 0.4 mm/rev led to increases of 65.28% and 147.93% in Ra, respectively. Additionally, compared to the 0.4 mm nose radius tool, the use of a 0.8 mm nose radius tool, which yielded the optimum surface quality, resulted in a 34.80% improvement in surface roughness.

**Keywords:** toolox 33, machine learning, heat map, decision tree, machinability

## 1. Introduction

Machining, as one of the fundamental pillars of metal-working technology, plays a vital role in transforming raw materials into final products with precise geometries. This category encompasses a range of processes, including turning, milling, drilling, and grinding, and is widely employed in the manufacturing of components requiring superior dimensional accuracy, superior surface finish, and complex geometries. In today's

manufacturing industry (particularly in sectors such as automotive, aerospace, mold making, and defense), enhancing the efficiency and sustainability of machining operations is of critical importance. At this stage, both the mechanical properties and the machinability of the workpiece material have a direct impact on the quality, duration, and cost of production. With the growing demand for high-performance steels in recent years, the Toolox series has increasingly drawn attention. Developed by the Swedish company SSAB, Toolox 33

\*Corresponding author:

Email: tayfuncetin@hakkari.edu.tr



© Author(s) 2025. This work is distributed under <https://creativecommons.org/licenses/by/4.0/>

Cite this article as:

Kaya, K. et.al. (2025). Finish turning of toolox 33 to improve machining parameters with different nose radius tools. *European Mechanical Science*, 9(3): 234-245. <https://doi.org/10.26701/ems.1724270>

History dates:

Received: 21.06.2025, Revision Request: 03.07.2025, Last Revision Received: 11.07.2025, Accepted: 27.07.2025



distinguishes itself with its pre-hardened and tempered structure. With a hardness of approximately 300 HB, it provides significant time and cost advantages by eliminating the need for post-machining heat treatment. Moreover, its high toughness, dimensional stability, and low internal stress levels make it a preferred choice in both mold manufacturing and machine component applications. However, while these advantageous mechanical properties improve performance, they also present challenges in terms of machinability (especially concerning tool wear and surface finish), necessitating careful optimization of cutting parameters. A systematic evaluation of the machinability characteristics of mold and tool steels is therefore essential for enhancing production efficiency and extending tool life. The machining of steels with superior mechanical properties, such as high hardness, toughness, and dimensional stability, requires not only the selection of appropriate cutting tool materials but also the precise adjustment of machining parameters. The following section presents a review of studies conducted on high-performance steels such as Toolox 44, 1.2367, and AISI P20, which exhibit similar structural and mechanical properties to Toolox 33.

Binali et al. [1] investigated the machinability of Toolox 44 hot-work tool steel, with a hardness of 44 HRC, using a dry milling process. In their experiments, they varied cutting speeds (150–240 m/min), feed rates (0.4–1.6 mm/tooth), and depths of cut (0.2–0.4 mm), evaluating cutting forces and surface quality. The results demonstrated that cutting parameters had an important influence, particularly on surface roughness and tool life. Despite the high hardness of Toolox 44, the findings indicated that its machinability could be enhanced under optimized cutting conditions. Persson et al. [2] compared the machinability of martensitic Toolox 33 and Toolox 44 steels with two commercial steels of similar hardness. Milling tests were conducted on samples with a hardness ranging from 300 to 400 HV30, focusing on tool life and wear behavior. Based on the Taylor machinability index, Toolox steels exhibited superior machinability at both hardness levels. The authors attributed this advantage to the influence of alloy composition on the tool wear mechanism. In a separate study, Binali et al. [3], studied the impacts of dry and minimum quantity lubrication (MQL) methods on the machinability of Nimax mold steel during milling. The evaluation considered criteria such as surface roughness, chip morphology, material removal rate, cutting temperature, and tool wear. Among the tested parameters, the MQL method was particularly effective in reducing tool wear and improving chip control. Although only limited improvements were observed in cutting temperature, MQL showed overall superiority over dry machining in terms of machinability performance. Bayraktar and Uzun [4] conducted an experimental comparison of the machinability of Nimax and Toolox 44 mold steels under three dissimilar feed rates and cutting speeds. Their results revealed that Toolox 44 generated higher cutting forces and surface roughness

than Nimax. While high cutting speed and low feed rate were optimal for Nimax, Toolox 44 performed better under low cutting speed and low feed rate. A rise in cutting speed led to significant increases in cutting force and surface roughness in Toolox 44, whereas these values decreased in Nimax. Surface analyses showed gap formation in Nimax and thermal deformation with more pronounced feed marks in Toolox 44. Kuram and Ucuncu [5] investigated the impacts of feed rate, tool nose radius, and cutting speed on tool wear and surface roughness during the dry turning of Toolox 44 steel, one of the commonly used machining methods. While no chip adhesion or crater wear was observed, flank wear was detected on the side surfaces of the inserts. The minimum tool wear occurred at a cutting speed of 140 m/min, a feed rate of 0.1 mm/rev, and a nose radius of 0.4 mm. The Ra value rises with feed rate and generally reduces with a larger nose radius. Based on their findings, the authors recommended avoiding a feed of 0.3 mm/rev and suggested using a nose radius of 0.8 mm at a feed of 0.2 mm/rev for advanced surface quality. Erdem et al. [6], examined the impacts of various machining parameters on surface roughness (Ra) and cutting forces during the turning of 1.2367 hot-work tool steel hardened to 55 HRC. The experimental design employed the Taguchi method, with three various feed rates, three cutting speeds, and a constant cutting depth. ANOVA was used to assess the effect of cutting parameters. The findings revealed that increasing the feed rate significantly raised the surface roughness, while cutting speed had no observable effect on Ra. Among the cutting forces (radial (Fx), tangential (Fy), and feed (Fz)), feed rate was found to be the most influential variable. In a related study, Özlü [7] conducted both experimental and statistical optimizations of machinability to minimize surface roughness ( $R_a$ ), vibration (Vib), cutting force ( $F_c$ ), energy consumption ( $E_c$ ), and during the dry turning of Toolox 44 steel. Experiments followed the Taguchi L27 design on a CNC lathe. Grey Relational Analysis (GRA) and ANOVA were applied to optimize multiple outputs simultaneously. The lowest measured energy consumption was 0.06 kW, and the optimal cutting parameter combination (220 m/min cutting speed, 0.1 mm/rev feed, and 0.5 mm depth of cut) was identified. According to GRA, the best parameter set was A1B3C1, and the overall improvement rate was calculated as 25.25%, confirming the success of the multi-criteria optimization. Binali et al. [8] analyzed the machinability of AISI P20 mold steel through milling simulations using the Finite Element Method (FEM). The study explored the influence of different speeds, feeds, and cutting depths on power consumption under up-milling and corner-milling strategies. Power was calculated using the resultant forces Fx, Fy, and Fz. The results showed that power consumption increased with all cutting parameters. The maximum and minimum power values were 8041.91 W and 1748.10 W, respectively, and the FEM predictions aligned well with experimental data. Kara [9] explored the influence of machining parameters on surface roughness during finish milling of AISI P20+S plastic

mold steel and identified optimal process parameters. The experiments were designed to utilize the Taguchi L8 orthogonal array, and the results were analyzed through signal-to-noise (S/N) ratios, ANOVA, and multiple regression analysis. The best surface quality was achieved at a cutting speed of 150 m/min, a feed of 0.1 mm/rev, a depth of cut of 0.16 mm, and under wet cooling conditions. The predicted and validated Ra values were 0.288  $\mu\text{m}$  and 0.296  $\mu\text{m}$ , respectively, with a model reliability of  $R^2 = 0.923$ . In another FEM-based study, Binali [10] examined the effects of different machining parameters on AISI P20 steel. Four cutting speeds, four feed rates, and two depths of cut were tested, with constant lateral feed. FEM simulations revealed that cutting force increased with higher cutting speed, feed, and cutting depth. Interestingly, when the cutting depth was kept constant, increasing the feed rate and cutting speed resulted in lower temperature values. Cutting forces ranged from 36.11 to 1951.42 N, and temperatures varied between 448.98 and 593.14  $^{\circ}\text{C}$ . These results demonstrated the effectiveness of FEM in optimizing machining parameters. Banavase et al. [11] investigate the effects of using vegetable oil as a high-pressure minimum quantity lubrication (MQL) fluid on tool life, chip morphology, and surface roughness during the turning of hardened Toolox<sup>®</sup> steel. Compared to conventional flood cooling, MQL—applied at varying pressures and flow rates—demonstrated significant improvements in tool performance and surface quality. The results highlight the potential of MQL systems in enhancing sustainability in machining processes and suggest further research opportunities across different operations, such as milling, drilling, and grinding. SK et al. [12] employ an artificial neural network (ANN) to predict flank wear based on cutting force and surface roughness during the turning of EN8 steel under dry conditions. Using a face-centered central composite design, the effects of cutting parameters and their interactions on machinability outputs were analyzed, revealing that feed rate had the most significant influence on surface roughness and tool wear. Among the tested training algorithms, the BFGS quasi-Newton backpropagation method yielded the lowest mean squared error with the shortest computation time. Elshaer et al. [13] focus on optimizing the turning parameters of TC21 titanium alloy, known for its high strength, toughness, and corrosion resistance, under both as-delivered and heat-treated conditions. Using a Taguchi L9 orthogonal array design, the effects of cutting speed, feed rate, and depth of cut on tool wear and surface roughness were evaluated. The results show that the three-stage heat treatment significantly improved machinability by reducing surface roughness by 56.25% and tool wear by 24.18%. Cutting speed and tool-workpiece contact time were the most influential factors. They also report that the depth of cut is the most influential parameter on surface roughness, accounting for 46.6% of its variability. Adizue et al. [14] explore the relationship between experimental design strategies, process optimization, and the prediction accuracy of machine learning models in ultra-precision

hard turning of 62 HRC AISI D2 steel using CBN inserts. Surface roughness and material removal rate were analyzed under Taguchi and full factorial designs, with a Bayesian regularized neural network (BRNN) employed for predictive modeling. The results demonstrated that the full factorial design improved prediction accuracy by 36% compared to the Taguchi method, with strong interpretability of machining parameters and high model reliability ( $R^2 = 0.99$ , MAPE = 8.14). Turan et al. [15] examine the influence of cutting tool coatings and machining parameters on surface roughness, cutting temperature, hole diameter accuracy, circularity, and cylindricity during the drilling of Al 6082-T6 alloy. Using a Taguchi L27 design, the predictive performances of Taguchi, artificial neural networks (ANN), and adaptive neuro-fuzzy inference system (ANFIS) models were compared based on both experimental data and corresponding S/N ratios. The ANN model demonstrated superior reliability and accuracy, particularly when using S/N-based data, and uncoated tools generally yielded better surface and dimensional outcomes, while TiAlN-coated tools were most effective in minimizing cylindricity error.

Although hot work tool steels have been widely investigated in the literature, studies specifically focusing on Toolox 33 remain relatively limited. In particular, there is a lack of systematic investigations into the behavior of this material under dry machining conditions, especially with regard to the influence of cutting parameters and tool geometry on surface quality and cutting forces. This study aims to comprehensively evaluate the machinability performance of Toolox 33 steel under dry turning conditions, focusing on the effects of tool nose radius, feed rate, depth of cut, and cutting speed. The novelty of the research lies in its systematic analysis of a relatively underexplored tool steel using a full factorial experimental design, along with the inclusion of machinability characterization specific to dry machining environments. In addition to conventional analysis techniques, machine learning-based approaches (decision tree analysis and heatmap correlation) were employed to assess the influence and interaction of machining parameters on output responses. The integration of these data-driven methods enables a deeper and more comprehensive understanding of the relationships between process parameters and machinability outcomes.

## 2. Materials and Methods

### 2.1. Workpiece Material, Cutting Tools, and Measurement Equipment

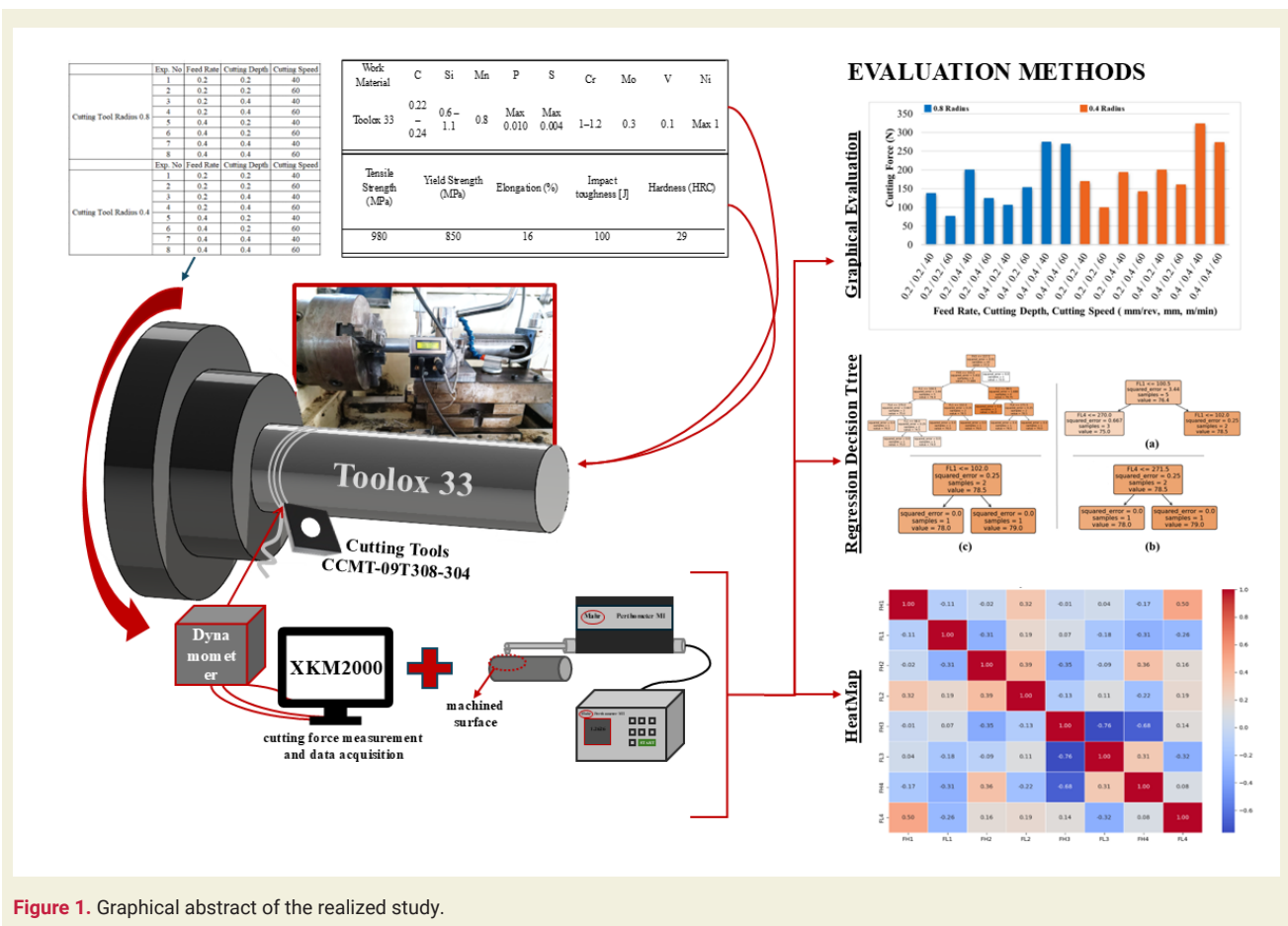
The Toolox 33 material used as the workpiece had a length of 200 mm and a diameter of 50 mm. ►Table 1 presents the chemical composition of the material, while ►Table 2 outlines its mechanical properties. The experiments were designed using a full factorial exper-

**Table 1.** Chemical composition of Toolox 33 (wt%)[16]

Work Material	C	Si	Mn	P	S	Cr	Mo	V	Ni
Toolox 33	0.22 – 0.24	0.6 – 1.1	0.8	Max 0.010	Max 0.004	1–1.2	0.3	0.1	Max 1

**Table 2.** Mechanical properties of Toolox 33

Tensile Strength (MPa)	Yield Strength (MPa)	Elongation (%)	Impact toughness [J]	Hardness (HRC)
980	850	16	100	29

**Figure 1.** Graphical abstract of the realized study.

imental approach, with three primary cutting parameters selected: feed rate (0.2–0.4 mm/rev), depth of cut (0.2–0.4 mm), and cutting speed (40–60 m/min). The cutting parameters applied in the experiments are presented in ►Table 3. All machining operations were performed on a conventional lathe under dry cutting conditions, without the use of any coolant.

Two carbide inserts (CCMT-09T308-304 and CCMT-09T304-304) with different nose radii were used as cutting tools. For each experimental setup, surface roughness ( $Ra_1$ – $Ra_{10}$ ) and cutting force ( $F_{c1}$ – $F_{c10}$ ) values were measured and recorded in Excel. Surface roughness was measured using a Mahr Perthometer M1 device, while cutting force values were captured using a TeLC dynamometer integrated into the lathe. Surface roughness values were determined in accordance with ISO 4287 by measuring the average surface roughness

( $Ra$ ) generated on the workpiece during machining. The calibration of the measurement instruments was performed using standard calibration equipment specifically designed for each device. These cutting force values were recorded in real time using the XKM2000 software. The recorded data were organized into tables, and average cutting force ( $F_{avg}$ ) values were calculated. ►Figure 1 presents a graphical summary of the experimental study.

## 2.2. Evaluation Methods

Initially, the variations in cutting force and surface roughness due to different machining parameter values considered in the study were examined through graphical analysis. In the second stage, machine learning methods were employed to further analyze the results. Python was used as the programming language for ma-



**Table 3.** Cutting parameters used in experiments

	Exp Nu.	Feed Rate (mm/rev)	Cutting Depth (mm)	Cutting Speed (m/min)
Cutting Tool Radius 0.8	1	0.2	0.2	40
	2	0.2	0.2	60
	3	0.2	0.4	40
	4	0.2	0.4	60
	5	0.4	0.2	40
	6	0.4	0.2	60
	7	0.4	0.4	40
	8	0.4	0.4	60
Cutting Tool Radius 0.4	1	0.2	0.2	40
	2	0.2	0.2	60
	3	0.2	0.4	40
	4	0.2	0.4	60
	5	0.4	0.2	40
	6	0.4	0.2	60
	7	0.4	0.4	40
	8	0.4	0.4	60

chine learning applications. Regression decision trees and heatmaps (used to visualize the correlation matrix) were selected as the primary machine learning methods in this study. In the study, the dataset was partitioned into training and testing subsets with an 80/20 split, and the decision tree algorithm was applied using its default parameters. Furthermore, Pearson correlation analysis was conducted to generate the heatmap.

Decision trees can be categorized into classification and regression types, depending on the nature of the data. Classification trees are used for discrete data, whereas regression trees handle continuous data. In a decision tree, the root node is the starting point from which data is split into branches, while the leaf node represents the final outcome where no further splitting occurs [17]. Each node is color-coded to represent purity, and numerical values in regression tree nodes facilitate the evaluation of results. The heatmap technique was employed to visualize the correlation matrix derived from the dataset. This method not only simplifies analysis for experts but also enhances the interpretability and accessibility of the findings for readers. Heatmaps distinguish between positive and negative correlations: in the case of a positive correlation, both variables tend to change in the same direction (either increasing or decreasing simultaneously), indicating a direct relationship. Shades of red represent positive correlations, whereas shades of blue denote negative correlations. Darker shades in either spectrum indicate stronger correlation levels [18].

### 3. Results and Discussions

The result parameters (surface roughness, cutting force) considered in this study are subjected to graphical evaluation, regression decision tree analysis, and heatmap interpretation under separate headings.

#### 3.1. Cutting Force

Cutting force is a mechanical response generated during machining and is one of the most critical output parameters, influencing tool condition, surface roughness, and overall surface quality [19]. When the workpiece material exhibits low machinability, cutting force values become significantly high during the process. As a result, tool wear may accelerate and tool life may be reduced [20, 21]. Additionally, increased cutting force can intensify machine vibrations, potentially causing considerable surface damage and leading to irregular surface profiles post-machining [22, 23]. Therefore, optimizing cutting force is essential for efficient machining processes. ► **Figure 2** illustrates the graphical distribution of the cutting force values obtained from the experiments. As depicted in the figure, the optimum cutting force was observed in the experiment conducted with a feed rate of 0.2 mm/rev, a cutting depth of 0.2 mm, and a cutting speed of 60 m/min, utilizing a tool with a tip radius of 0.8 mm. When using a cutting tool with a 0.4 mm nose radius under the machining parameters that yielded the optimum results, a 29.87% increase in cutting force values was observed. A general analysis reveals that high feed rates and cutting depths, in addition to both low and high cutting speeds, contributed to increased cutting forces for both tool tip radius. In the experimental setup where the feed rate was 0.2 mm/rev, the depth of cut was 0.2 mm, the cutting speed was 60 m/min, and a cutting tool with a 0.8 mm nose radius was used, increasing the feed rate to 0.4 mm/rev resulted in a 100% increase in cutting force. Additionally, under the same cutting conditions, increasing the depth of cut from 0.2 mm to 0.4 mm led to a 62.33% increase in cutting force. In the 0.8 mm tip radius test set (except for the experiment conducted with 0.2 mm/rev feed, 0.4 mm cutting depth, and 40 m/min cutting speed), cutting forces were lower compared to those in the 0.4 mm tip radius test set. This reduction in cutting force with increased tip radius can be attributed to more stable cutting due to reduced vibration (resulting from enhanced tool rigidity) or the improved thermal distribution over a larger contact area, which facilitates the cutting process. Cutting force values also decreased with growing cutting speed. In the experimental setup where the feed rate was 0.2 mm/rev, the depth of cut was 0.2 mm, and the tool nose radius was 0.8 mm, increasing the cutting speed from 40 m/min to 60 m/min resulted in a 44.20% reduction in cutting force. This reduction may be associated with the thermal softening of the material due to heat buildup at higher speeds, which alters the mechanical properties of the cork material or enhances plastic deformation, making the cut-

ting process easier [24, 25]. However, in the test with a 0.8 mm tip radius, 0.4 mm/rev feed, 0.2 mm cutting depth, and cutting speeds increased from 40 m/min to 60 m/min, cutting forces were observed to rise. This can be explained by the inability of the large chip section—formed due to the high feed rate and large tip radius—to undergo sufficient thermal softening, resulting in higher resistance in the machining zone. A comparable finding was documented in [26]. The increase in cutting force with feed rate (from 0.2 mm/rev to 0.4 mm/rev) is attributed to a larger chip load and insufficient chip evacuation [27], consistent with findings in the literature [28–30]. Interestingly, in the experiment with a 0.8 mm tip radius, 0.2 mm depth of cut, and 40 m/min cutting speed, cutting forces decreased with increased feed rate. This anomaly may be due to a larger cutting contact area and higher heat generation, making the material easier to cut. As cutting depth increases, so do cutting forces. This is due to the increased resistance resulting from a larger cutting area, which requires more power for material removal [31, 32]. The highest cutting force was observed with the 0.4 mm tip radius tool, using 0.4 mm/rev feed, 0.4 mm cutting depth, and 40 m/min speed.

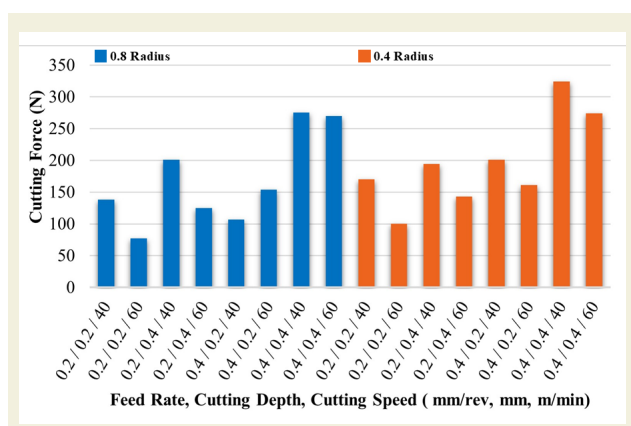


Figure 2. Graphical representation of cutting force value.

► **Figure 3** shows the regression decision tree for cutting force. In the figure, “H” denotes a 0.8 mm tip radius and “L” denotes a 0.4 mm tip radius. In ► **Figure 3a**, the cutting force values from the experiments with a 0.4 mm tip radius, 0.2 mm/rev feed, and 0.2 mm cutting depth at 40 m/min and 60 m/min cutting speeds correspond to nodes with values of 78.5 and 75, respectively. Based on this, it can be concluded that cutting force values decrease as cutting speed values increase. ► **Figure 3b** compares results from the same tool radius and cutting depth (0.4 mm) and constant cutting speed (40 m/min), where increasing the feed rate from 0.2 to 0.4 mm/rev increased the value from 78 to 79, indicating a rise in cutting force. In ► **Figure 3c**, with constant tool radius (0.4 mm), feed (0.2 mm/rev), and speed (60 m/min), escalating the cutting depth from 0.2 to 0.4 mm also increased the cutting force from 78 to 79. These observations confirm that cutting force increases with both cutting depth and feed rate. The consistency between the regression tree and graphical evaluations

strengthens the reliability and accuracy of the experimental findings.

► **Figure 4** presents the heatmap of cutting force. The dark red squares along the diagonal indicate the highest positive correlations within the same parameters. In the figure, positive correlations are depicted in various shades of red, whereas negative correlations are shown in different shades of blue. As in the decision tree, “H” and “L” denote 0.8 mm and 0.4 mm tip radii, respectively. According to the figure, the strongest positive correlation was observed between FH1 and FL4. FH1 used parameters of 0.2 mm/rev feed rate, 0.2 mm cutting depth, and 40 m/min speed, while FL4 used 0.2 mm/rev feed, 0.4 mm depth of cut, and 60 m/min speed. In both cases, cutting forces increased with cutting depth and speed, suggesting that the cutting depth had the most crucial positive correlation with cutting force. A notable negative correlation occurred between FH3 and FH4, where feed and cutting depth were constant, but cutting force decreased with increased cutting speed. This again highlights the inverse relationship between cutting speed and cutting force. A positive correlation exists between cutting force and depth of cut is likely the strongest due to the pronounced effect of increased material resistance at higher cutting depths.

### 3.2. Surface Roughness

Surface roughness is a result of the mechanical engagement between the cutting tool and the surface of the work material. To attain a high-quality final surface profile, surface roughness values must remain minimal, which can be accomplished through proper optimization of the machining parameters [33]. ► **Figure 5** presents the graphical representation of the surface roughness data obtained from the experiments. As observed, the 0.8 mm tip radius yielded more favorable results in achieving optimal surface roughness compared to the 0.4 mm tip radius. Thus, a larger tip radius positively influenced surface roughness. Compared to the experiment conducted with a 0.4 mm nose radius tool, the use of a 0.8 mm nose radius tool, which yielded the optimum surface roughness, resulted in a 34.80% reduction in surface roughness. The impact of speed on surface roughness was not uniform across all test conditions. When the cutting speed increased from 40 to 60 m/min, surface roughness (Ra) values decreased on average by approximately 5% to 22%, while in some cases, a slight increase of up to 3% was observed. A growth in cutting speed may result in reduced surface roughness due to the associated rise in temperature within the machining zone, which in turn reduces friction between the tool and the chip and enhances chip evacuation [34, 35]. However, an increase in surface roughness with higher cutting speeds may also occur due to the accelerated wear of the cutting tool [36]. In all experimental sets, an rise in feed rate causes a consistent increase in surface roughness, which aligns with prior studies [37, 38]. This phenomenon can be attributed to the larger volume of material removed per unit time, which in-

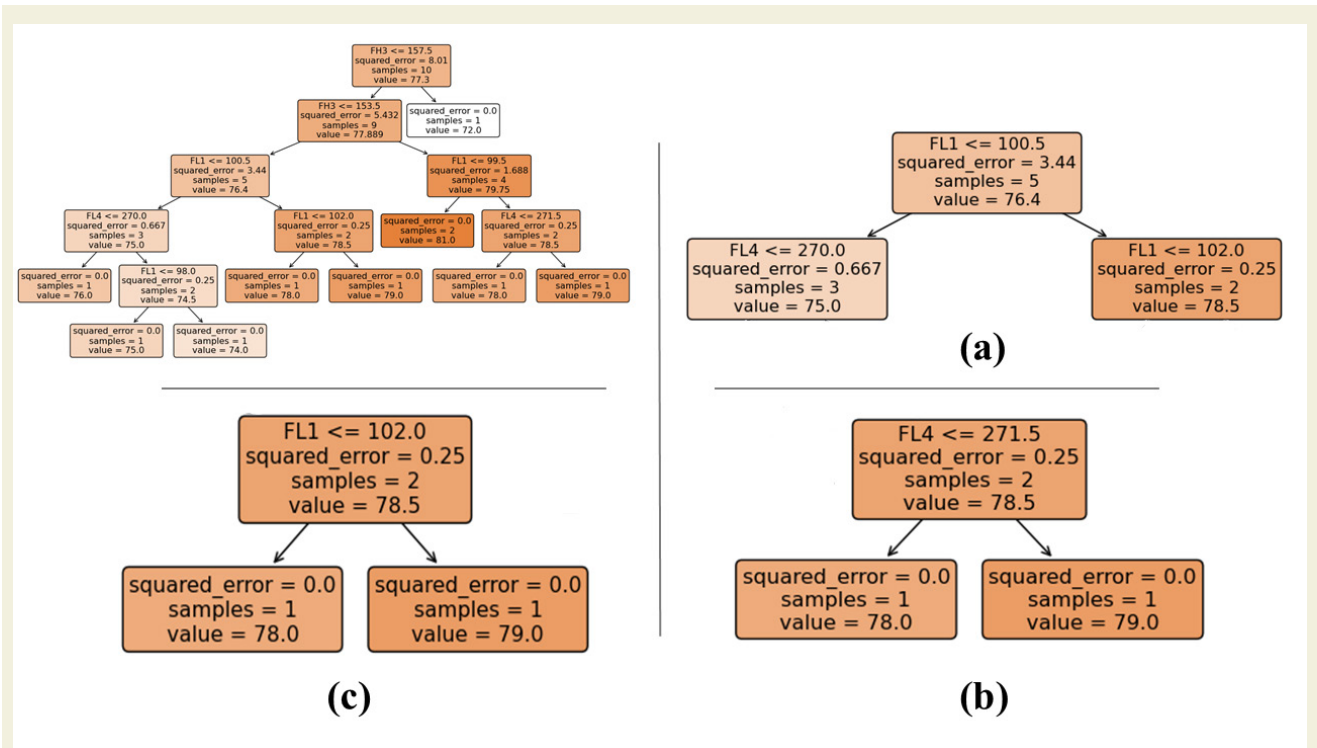


**Figure 3.** Regression decision tree model for cutting force parameter.

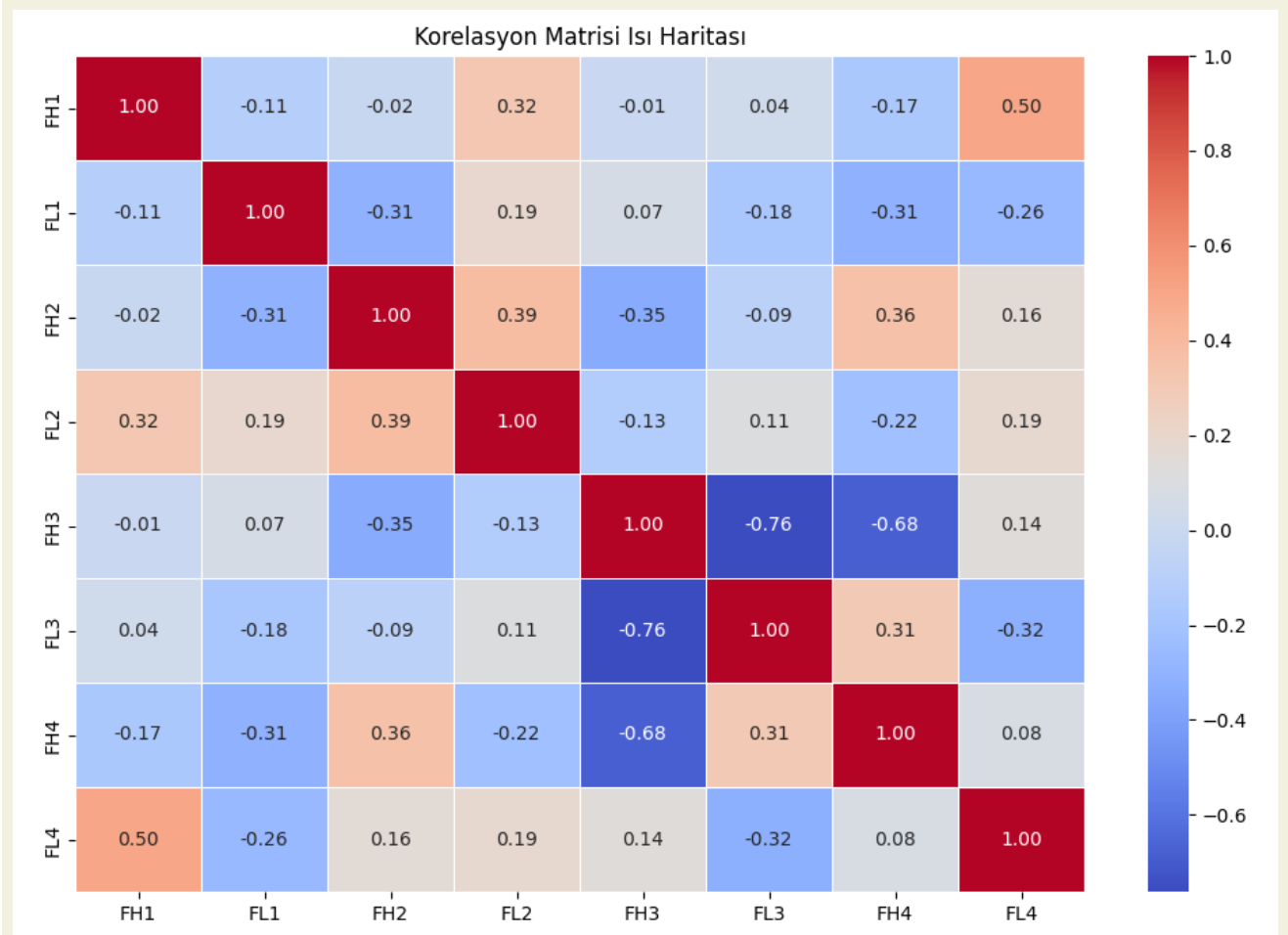


**Figure 4.** Heat map model for cutting force parameter.

creases deformation on the surface. Similarly, surface roughness values increased with greater cutting depth, a result frequently reported in the literature. In the experimental setup using a cutting tool with a 0.8 mm nose radius, where optimum surface roughness values were achieved, increasing the depth of cut from 0.2 mm to 0.4 mm resulted in a 65.28% increase in surface roughness. This phenomenon is primarily due to the increased chip volume and enhanced friction between the cutting tool and the workpiece surface [39]. In the experimental setup using a cutting tool with a 0.8 mm nose radius, where optimum surface roughness values were obtained, increasing the feed rate from 0.2 mm/rev to 0.4 mm/rev caused a 147.93% increase in surface roughness. However, an exception was noted in the test conducted with a tool tip radius of 0.8 mm, a feed of 0.4 mm/rev, and a cutting speed of 40 m/min. In this case, increasing the depth of cut from 0.2 mm to 0.4 mm led to a reduction in surface roughness. This arises from the concentration of plastic deformation in the cutting direction, which reduced lateral flow and surface defects, stabilized the cutting process, and minimized vibration—collectively resulting in improved surface finish. The minimum surface roughness was observed in the experiment conducted with a 0.8 mm tip radius, 60 m/min cutting speed, 0.2 mm depth of cut, and 0.2 mm/rev feed. Conversely, the maximum surface roughness occurred with a 0.4 mm tip radius, 0.4 mm/rev feed, 0.4 mm cutting depth, and 40 m/min cutting speed.

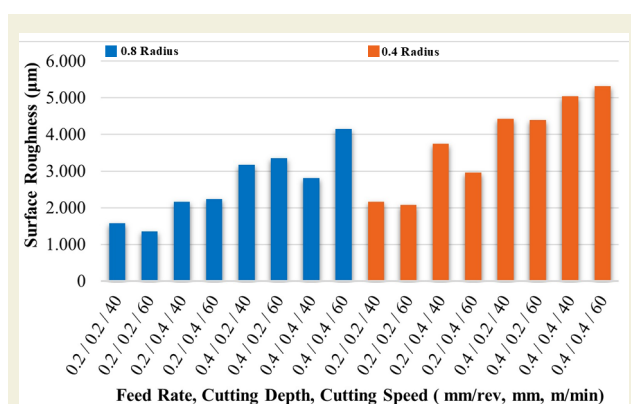


Figure 5. Graphical representation of surface roughness values.

► **Figure 6** displays the regression decision tree developed for surface roughness. As with the decision tree for cutting force, the letter H denotes a 0.8 mm tip radius, while L indicates a 0.4 mm tip radius. In ► **Figure 6a**, both increasing and decreasing trends in surface roughness due to cutting speed are evident. Specifically, in the experiments conducted with a 0.8 mm tip radius tool, the cutting speed of 40 m/min corresponds to a node value of 9, while 60 m/min corresponds to a value of 8. This decrease suggests that higher cutting speeds may reduce surface roughness. Thus, the model confirms that cutting speed may have both positive and negative impacts on surface roughness depending on the conditions. In ► **Figure 6b**, experiments with a 0.4 mm tip radius tool and varying feed rates show that the

lower feed rate corresponds to a node value of 2, while the higher feed rate corresponds to 3.5. This reflects the trend seen in the graphical evaluation, where surface roughness increased with higher feed rates. ► **Figure 6c** presents results for the 0.8 mm tip radius tool under different cutting depths. The lower depth of cut correlates with a node value of 0.5 and the higher depth with a value of 3, reaffirming the graphical analysis: surface roughness increases with greater cutting depth. The regression tree results closely match the graphical evaluations, reinforcing the validity and accuracy of the machine learning model.

► **Figure 7** presents the heatmap for surface roughness correlations. Shades of red correspond to positive correlations, while shades of blue represent negative correlations, and darker tones in both colors signify stronger correlations. As in the decision tree, H denotes tests with a 0.8 mm tip radius, while L denotes those with 0.4 mm. The strongest positive correlation was observed between RaH3 and RaH1. In these experiments, increases in both cutting depth and cutting speed led to higher surface roughness, suggesting a direct relationship among these parameters. A similar positive correlation was observed between RaL1 and RaL4. The most significant negative correlation appeared between RaL4 and RaH2. Another strong negative correlation was found between RaL2 and RaL3, indicating that surface roughness increased as cutting speed decreased. These results confirm that cutting speed can have varying impacts on surface roughness depending on the experimental conditions, consistent with the graphical and decision tree evaluations.

## 4. Conclusions

The current research, the impacts of varying independent variables on cutting force and surface roughness in the course of dry turning of Toolox 33 material, was investigated in order to assess the machinability of the workpiece material. The key findings are summarized below:

- The cutting tool with a 0.8 mm tip radius demonstrated more efficient performance in machining Toolox 33 compared to the 0.4 mm tip radius tool, yielding optimal results in terms of both force and roughness.
- Cutting force values decreased with ascending cutting speed, while increases in feed rate and depth of cut led to higher forces.
- Surface roughness exhibited both increasing and decreasing trends with speed changes. However, increases in feed and depth of cut consistently hurt surface quality, leading to increased surface roughness values.
- The results obtained from machine learning meth-



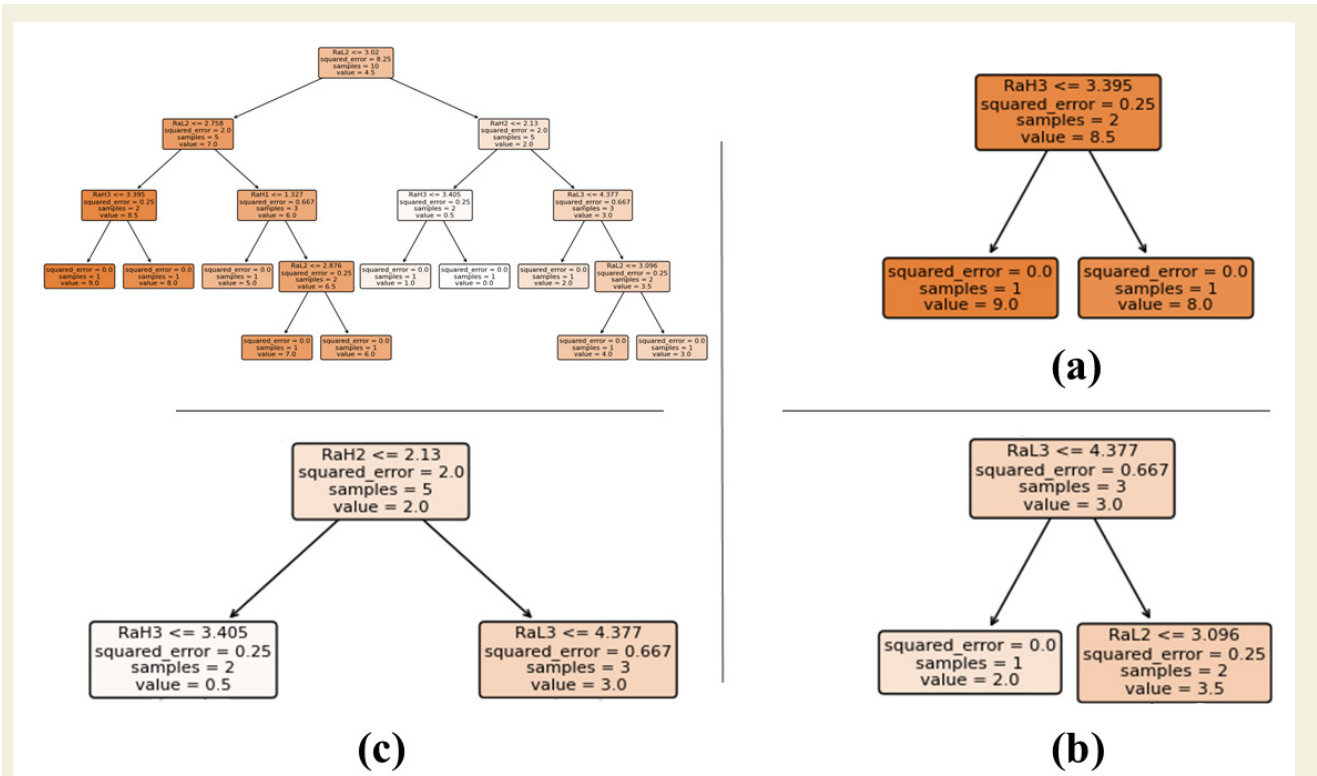


Figure 6. Regression decision tree model for surface roughness parameter.

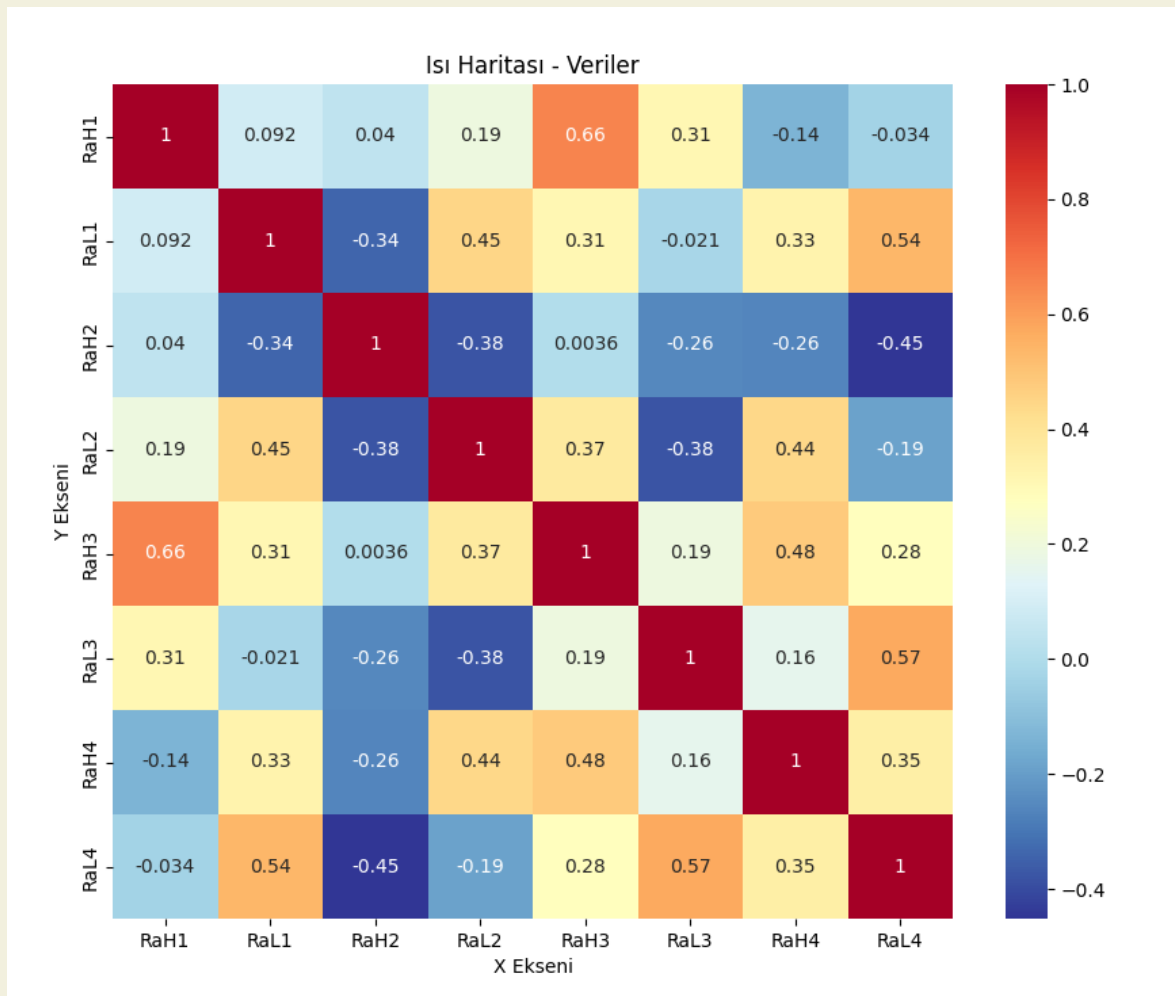


Figure 7. Heat map model for surface roughness parameter.

ods (regression decision trees and heatmaps) corresponded well with the findings from graphical evaluations for both cutting force and roughness.

- Using a tool with a 0.8 mm nose radius as the baseline optimum condition, a reduction in nose radius to 0.4 mm caused the cutting force to rise by 29.87%. Increasing the feed rate to 0.4 mm/rev doubled the cutting force, while raising the depth of cut to 0.4 mm led to a 62.33% increase. Conversely, elevating the cutting speed from 40 m/min to 60 m/min resulted in a 44.20% decrease in cutting force.
- Physical testing revealed that raising the cutting speed from 40 to 60 m/min contributed to a reduction in surface roughness (Ra) ranging between approximately 5% and 22%. In contrast, increasing the cutting depth from 0.2 mm to 0.4 mm and the feed rate from 0.2 mm/rev to 0.4 mm/rev caused Ra to increase by 65.28% and 147.93%, respectively. Furthermore, the application of a tool with a 0.8 mm nose radius—compared to a 0.4 mm radius tool—achieved optimal surface finish, improving surface roughness by 34.80%.
- In future studies, it is anticipated that machine learning techniques, particularly decision tree algorithms and heatmaps, will be increasingly employed for the optimization of cutting parameters in machinability research. In real-time and multi-variate manufacturing environments, these methods will enable more effective analysis of the effects of process parameters on outputs such as surface quality, cutting force, and tool life. The integration of visualization tools like heatmaps and correlation analyses will facilitate the understanding of complex relationships among parameters and improve model accuracy. Consequently, data-driven decision support systems will be developed for manufacturing processes, enhancing both the speed and precision of machinability evaluations. Ultimately, machine learning-based approaches will play a crucial role in optimizing cutting parameters and improving process efficiency, offering significant quality and cost benefits in advanced manufacturing technologies.

## Acknowledgments

This research was supported by Hakkari University, Scientific Research Project Coordination Unit (BAP; Grant no. FM24BAP8).

## Research ethics

Not applicable.

## Artificial Intelligence Use

The author(s) declare that no generative artificial intelligence (e.g., ChatGPT, Gemini, Copilot, etc.) was used in any part of this study.

## Author contributions

Conceptualization: [Tayfun Çetin], Methodology: [Rüstem Binali], Formal Analysis: [Kübra Kaya], Investigation: [Tayfun Çetin], Resources: [Tayfun Çetin], Data Curation: [Rüstem Binali], Writing - Original Draft Preparation: [Kübra Kaya, Tayfun Çetin], Writing - Review & Editing: [Tayfun Çetin, Kübra Kaya, Rüstem Binali, Hakan Gündoğmuş], Visualization: [--], Supervision: [Hakan Gündoğmuş], Project Administration: [Hakan Gündoğmuş], Funding Acquisition: [Hakan Gündoğmuş]

## Competing interests

The author(s) state(s) no conflict of interest.

## Research funding

This research was supported by Hakkari University, Scientific Research Project Coordination Unit (BAP; Grant no. FM24BAP8).

## Data availability


Not applicable.

## Peer-review

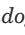
Externally peer-reviewed.

## Orcid

Kübra Kaya  <https://orcid.org/0000-0002-9971-8826>

Tayfun Çetin  <https://orcid.org/0009-0003-3089-0489>

Rüstem Binali  <https://orcid.org/0000-0003-0775-3817>

Hakan Gündoğmuş  <https://orcid.org/0000-0003-4118-0207>

## References

- [1] Binali, R., Demir, H., & Çiftçi, İ. (2017). An investigation into the machinability of hot work tool steel (Toolox 44). 3rd Iron and Steel Symposium (UDCS'17), 441-444.
- [2] Persson, U., & Chandrasekaran, H. (2002). Machinability of martensitic steels in milling and the role of hardness. In Proc. 6th Int. Tooling Conf., Karlstad University, Sweden, 1225-1236.
- [3] Binali, R., Demirpolat, H., Kuntoğlu, M., & Sağlam, H. (2023). Machinability investigations based on tool wear, surface roughness, cutting temperature, chip morphology and material removal rate during dry and MQL-assisted milling of Nimax mold steel. *Lubricants*, 11(3), 101. <https://doi.org/10.3390/lubricants11030101>
- [4] Bayraktar, Ş., & Uzun, G. (2021). Ön sertleştirilmiş Toolox 44 ve Nimax kalıp çeliklerinin işlenebilirliği üzerine deneysel çalışma. *Gazi Üniversitesi Mühendislik Mimarlık Fakültesi Dergisi*, 36(4), 1939-1948. <https://doi.org/10.17341/gazimmfd.641824>

- [5] Kuram, E., & Ucuncu, N. (2024). Toolox 44 çeliğinin tormalanmasında kesme hızının, ilerlemenin ve kesici uç burun radyüsünün takım aşınmasına ve yüzey pürüzlülüğüne etkileri. *Gazi Üniversitesi Fen Bilimleri Dergisi Part C: Tasarım ve Teknoloji*, 12(4), 1006-1017. <https://doi.org/10.29109/gujsc.1530456>
- [6] Erdem, S., Özdemir, M., Rafighi, M., & Yavuz, M. (2023). 1.2367 sıcak iş takım çeliğinin sert tormalanmasında kesme parametrelerinin yüzey pürüzlülüğü ve kesme kuvvetleri üzerinde etkisi. *Politeknik Dergisi*, 26(3), 1071-1077. <https://doi.org/10.2339/politeknik.1059568>
- [7] Özlü, B. (2022). Evaluation of energy consumption, cutting force, surface roughness and vibration in machining Toolox 44 steel using Taguchi-based gray relational analysis. *Surface Review and Letters*, 29(08). <https://doi.org/10.1142/S0218625X22501037>
- [8] Binali, R., Coşkun, M., & Neşeli, S. (2022). An investigation of power consumption in milling AISI P20 plastic mold steel by finite elements method. *Avrupa Bilim ve Teknoloji Dergisi*, (34), 513-518. <https://doi.org/10.31590/ejosat.1083257>
- [9] Plastike, M. (2018). Optimization of surface roughness in finish milling of AISI P20+ S plastic-mold steel. *Optimization*, 52(2), 195-200. <https://doi.org/10.17222/mit.2017.088>
- [10] Binali, R. (2023). Parametric optimization of cutting force and temperature in finite element milling of AISI P20 steel. *Journal of Materials and Mechatronics: A*, 4(1), 244-256. <https://doi.org/10.55546/jmm.1257453>
- [11] Banavase Shivalingappa, A., & Dhamal, A. C. (2019). Analysis of machining performance using high pressure minimum quantity lubrication (MQL) [Master's thesis, KTH, School of Industrial Engineering and Management (ITM), Sweden].
- [12] S. K., T., Shankar, S., & K. D. (2020). Tool wear prediction in hard turning of EN8 steel using cutting force and surface roughness with artificial neural network. *Proceedings of the Institution of Mechanical Engineers, Part C: Journal of Mechanical Engineering Science*, 234(1), 329-342. <https://doi.org/10.1177/0954406219873932>
- [13] Elshaer, R. N., El-Aty, A. A., Sayed, E. M., Barakat, A. F., & Sobh, A. S. (2024). Optimization of machining parameters for turning operation of heat-treated Ti-6Al-3Mo-2Nb-2Sn-2Zr-1.5 Cr alloy by Taguchi method. *Scientific Reports*, 14(1). <https://doi.org/10.1038/s41598-024-65786-8>
- [14] Adizue, U. L., & Takács, M. (2025). Exploring the correlation between design of experiments and machine learning prediction accuracy in ultra-precision hard turning of AISI D2 with CBN insert: A comparative study of Taguchi and full factorial designs. *The International Journal of Advanced Manufacturing Technology*, 137, 2061-2090. <https://doi.org/10.1007/s00170-025-15186-7>
- [15] Turan, İ., Özlü, B., Ulaş, H. B., & Demir, H. (2025). Prediction and modelling with Taguchi, ANN and ANFIS of optimum machining parameters in drilling of Al 6082-T6 alloy. *Journal of Manufacturing and Materials Processing*, 9(3), 92. <https://doi.org/10.3390/jmmp9030092>
- [16] Hernandez, S., Hardell, J., Winkelmann, H., Ripoll, M. R., & Prakash, B. (2015). Influence of temperature on abrasive wear of boron steel and hot forming tool steels. *Wear*, 338, 27-35. <https://doi.org/10.1016/j.wear.2015.05.010>
- [17] Bansal, M., Goyal, A., & Choudhary, A. (2022). A comparative analysis of K-nearest neighbor, genetic, support vector machine, decision tree, and long short term memory algorithms in machine learning. *Decision Analytics Journal*, 3, Article 100071. <https://doi.org/10.1016/j.dajour.2022.100071>
- [18] Jumasseitova, A. K., & Kaidarova, N. A. (2024). Understanding management challenges through heatmap analysis of online teaching experience correlations. *Annali d'Italia*, 60, 29-36.
- [19] Liu, M., Xie, H., Pan, W., Ding, S., & Li, G. (2025). Prediction of cutting force via machine learning: State of the art, challenges and potentials. *Journal of Intelligent Manufacturing*, 36(2), 703-764. <https://doi.org/10.1007/s10845-023-02260-8>
- [20] Li, G., Li, N., Wen, C., & Ding, S. (2018). Investigation and modeling of flank wear process of different PCD tools in cutting titanium alloy Ti6Al4V. *The International Journal of Advanced Manufacturing Technology*, 95, 719-733. <https://doi.org/10.1007/s00170-017-1222-0>
- [21] Ma, J., Gao, Y., Jia, Z., Song, D., & Si, L. (2018). Influence of spindle speed on tool wear in high-speed milling of Inconel 718 curved surface parts. *Proceedings of the Institution of Mechanical Engineers, Part B: Journal of Engineering Manufacture*, 232(8), 1331-1341. <https://doi.org/10.1177/0954405416668925>
- [22] Arnaud, L., Gonzalo, O., Seguy, S., Jauregi, H., & Peigné, G. (2011). Simulation of low rigidity part machining applied to thin-walled structures. *The International Journal of Advanced Manufacturing Technology*, 54, 479-488. <https://doi.org/10.1007/s00170-010-2976-9>
- [23] Li, G., Yi, S., Li, N., Pan, W., Wen, C., & Ding, S. (2019). Quantitative analysis of cooling and lubricating effects of graphene oxide nanofluids in machining titanium alloy Ti6Al4V. *Journal of Materials Processing Technology*, 271, 584-598. <https://doi.org/10.1016/j.jmatprotec.2019.04.035>
- [24] Gökçaya, H., & Nalbant, M. (2007). Kesme hızının yığıntı katmanı ve yığıntı talaş oluşumu üzerindeki etkilerinin SEM ile incelenmesi. *Gazi Üniversitesi Mühendislik Mimarlık Fakültesi Dergisi*, 22(3), 481-488.
- [25] Hekimoğlu, A. P., Bayraktar, Ş., & Turgut, Y. (2018). Kesme hızı ve ilerlemenin Al-35Zn alaşımının işlenebilirliğine etkisinin incelenmesi. In *SETSci-Conference Proceedings (Vol. 3, pp. 77-83)*.
- [26] Korkut, İ., & Donertas, M. A. (2007). The influence of feed rate and cutting speed on the cutting forces, surface roughness and tool-chip contact length during face milling. *Materials & Design*, 28(1), 308-312. <https://doi.org/10.1016/j.matdes.2005.06.002>
- [27] Binali, R., Demirpolat, H., Kuntoğlu, M., & Kaya, K. (2024). Exploring the tribological performance of mist lubrication technique on machinability characteristics during turning S235JR steel. *Manufacturing Technologies and Applications*, 5(3), 276-283. <https://doi.org/10.52795/mateca.1541090>
- [28] Aydın, M. (2024). Ti6Al4V alaşımının ortogonal tormalanmasında ilerleme hızının kesme kuvveti ve talaş morfolojisi üzerindeki etkilerinin sonlu elemanlar analizi. *Gazi University Journal of Science Part C: Design and Technology*, 12(2), 567-576. <https://doi.org/10.29109/gujsc.1420233>
- [29] Yılmaz, V., Dilipak, H., Sarıkaya, M., Yılmaz, C. Y., & Özdemir, M. (2014). Frezeleme işlemlerinde kesme kuvveti, titreşim ve yüzey pürüzlülüğü sonuçlarının modellenmesi. *Erciyes Üniversitesi Fen Bilimleri Enstitüsü Fen Bilimleri Dergisi*, 30(4), 220-226.
- [30] Şeker, U., Kurt, A., & Ciftci, İ. (2004). The effect of feed rate on the cutting forces when machining with linear motion. *Journal of Materials Processing Technology*, 146(3), 403-407. <https://doi.org/10.1016/j.jmatprotec.2003.12.001>
- [31] Demirpolat, H., Binali, R., Patange, A. D., Pardeshi, S. S., & Gnasekaran, S. (2023). Comparison of tool wear, surface roughness, cutting forces, tool tip temperature, and chip shape during sustainable turning of bearing steel. *Materials*, 16(12), 4408. <https://doi.org/10.3390/ma16124408>
- [32] Demirpolat, H., Kaya, K., Binali, R., & Kuntoğlu, M. (2023). AISI 52100 rulman çeliğinin tormalanmasında işleme parametrelerinin yüzey pürüzlülüğü, kesme sıcaklığı ve kesme kuvveti üzerindeki etkilerinin incelenmesi. *İmalat Teknolojileri ve Uygulamaları*, 4(3), 179-189. <https://doi.org/10.52795/mateca.1393430>
- [33] Memiş, F. (2015). AISI 2205 (EN 1.4462) paslanmaz çeliğin CNC torna tezgahında işlenmesinde yüzey pürüzlülüğü ve kesme kuvvetlerinin deneysel araştırılması [Master's thesis, Fen Bilimleri Enstitüsü].
- [34] Trent, E. M., & Wright, P. K. (1991). *Metal cutting* (3rd ed.). Butterworth-Heinemann.
- [35] Kul, B. S., & Yamaner, A. S. Comparative evaluation of dry-MQL turning applications for AISI 5115 steel. *Manufacturing Technologies and Applications*, 6(1), 23-32.
- [36] Akgün, M., Özger, G., & Ulaş, H. B. (2014). Döküm yöntemiyle üretilmiş AZ91 magnezyum alaşımının işlenebilirliğinin yüzey pürüzlülüğü açısından değerlendirilmesi. *Erciyes Üniversitesi Fen Bilimleri Enstitüsü Fen Bilimleri Dergisi*, 30(5), 323-328.
- [37] Kuntoğlu, M., Kaya, K., & Binali, R. (2023). Investigation of surface roughness changes in the machining of carbon steel under sustainable conditions. In *1st International Conference on Pioneer and*

- Innovative Studies (pp. 163-167).
- [38] Yamaner, A. S., & Kul, B. S. (2025). Evaluation of tool radius and machining parameters on cutting forces and surface roughness for AA 6082 aluminum alloy. *European Mechanical Science*, 9(2), 125-138. <https://doi.org/10.26701/ems.1666294>
- [39] Demir, H., Ulaş, H. B., & Binali, R. (2018). Toolox 44 malzemesinde talaş kaldırma miktarının yüzey pürüzlülüğü ve takım aşınması üzerindeki etkilerinin incelenmesi. *Technological Applied Sciences*, 13(1), 19-28. <https://doi.org/10.12739/NWSA.2018.13.1.2A0132>